

Design, synthesis, and SAR analysis of novel selective σ_1 ligands

Simona Collina,^{a,*} Guya Loddo,^a Mariangela Urbano,^a Laura Linati,^b
Athos Callegari,^c Francesco Ortuso,^d Stefano Alcaro,^d Christian Laggner,^e
Thierry Langer,^e Orazio Prezzavento,^f Giuseppe Ronsisvalle^f and Ornella Azzolina^a

^a*Dipartimento di Chimica Farmaceutica, Università di Pavia, Viale Taramelli 12, 27100 Pavia, Italy*

^b*Centro Grandi Strumenti, Università di Pavia, Via Bassi 21, 27100 Pavia, Italy*

^c*Dipartimento di Scienze della Terra, Università degli Studi di Pavia, Via Ferrata 1, 27100 Pavia, Italy*

^d*Dipartimento di Scienze Farmacologiche 'Complesso Nini Barbieri' Università di Catanzaro 'Magna Graecia',
88021 Roccelletta di Borgia (CZ), Italy*

^e*Department of Pharmaceutical Chemistry and Center for Molecular Biosciences (CMBI), University of Innsbruck,
A-6020 Innsbruck, Austria*

^f*Dipartimento di Scienze Farmaceutiche, Università di Catania, Viale A. Doria 6, 95125 Catania, Italy*

Received 8 September 2006; revised 18 October 2006; accepted 23 October 2006

Available online 25 October 2006

Abstract—A new series of arylalkyl- and alkenylamines was designed, synthesized, and evaluated for binding to σ_1 and σ_2 receptors. Many compounds exhibited nanomolar affinity for σ_1 subtype receptor with good selectivity over σ_2 . A molecular modeling study was conducted in order to rationalize the experimental data, and the structure-receptor affinities are discussed.

© 2006 Elsevier Ltd. All rights reserved.

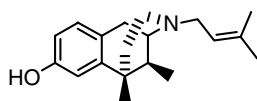
1. Introduction

Although sigma receptors were discovered about 30 years ago as a subtype of opioid receptors, the importance of their biological properties is not yet completely clarified.^{1,2} At present it is accepted that sigma receptors are a unique family of proteins different from opioid and *N*-methyl-D-aspartate (NMDA) phencyclidine receptors.³ The sigma receptors bind numerous xenobiotics of unrelated classes of compounds (Fig. 1) such as many clinical drugs used in psychiatric disorders including haloperidol, imipramine, and selective serotonin reuptake inhibitors.² Pharmacological studies have identified two distinct subtypes of sigma receptor, namely σ_1 and σ_2 , which are expressed in various areas of the brain and in peripheral organs.^{4–7} The σ_1 subtype, classified as a typical membrane receptor, can be considered an important intracellular regulatory protein since it can be translocated, when activated, from the endoplasmic reticulum, where it is present under resting conditions.⁸ Many trans-

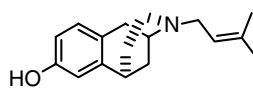
duction systems, such as the glutamatergic, cholinergic, and catecholaminergic systems, are sensitive to σ_1 -mediated neuromodulation.⁹ The σ_1 receptor has been cloned, and the purified protein is a 25–30 kDa single polypeptide characterized by a single transmembrane domain anchored in mitochondrial membranes and endoplasmic reticulum.¹⁰ The deduced amino acid sequence of the purified protein, seemingly correspondent to σ_1 receptor, does not resemble that of any known mammalian protein. Progesterone has been suggested to be a possible endogenous ligand, since it was found to inhibit tritiated (+)-SKF10,047 ((+)-*N*-allylnormetazocine) binding in rat brain at nanomolar concentrations.¹¹ However, other steroids, such as pregnenolone, dehydroepiandrosterone (DHEA), and testosterone, have moderate affinity. Pregnenolone and DHEA activate the σ_1 protein, while progesterone is the most potent inactivator.¹² Thus, sigma receptors could mediate some aspects of steroid-induced mental disturbances and may have neuroprotective properties.¹³ Since endogenous ligands for the σ_1 receptor have not yet been identified and its physiological function is still to be wholly elucidated, it might be better defined σ_1 protein. Likewise, it may be better to consider its role as an activator/inactivator rather than agonist/antagonist.

Keywords: Arylalkylamines; Sigma receptors; Molecular modeling; SAR studies.

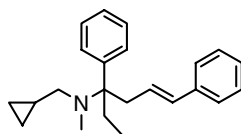
* Corresponding author. Tel.: +39 382 987376; fax: +39 382 422975;
e-mail: simona.collina@unipv.it

(+)-Pentazocine

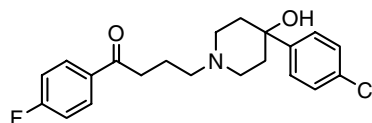
(+)-1,2,3,4,5,6-Hexahydro-6,11-dimethyl-3-(3-methyl-2-butenyl)-2,6-methano-3-Benzazocin-8-ol

SKF 10,047

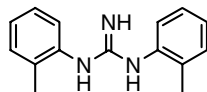
(+)-1,2,3,4,5,6-Hexahydro-3-(3-methyl-2-butenyl)-2,6-methano-3-Benzazocin-8-ol

Igmesine

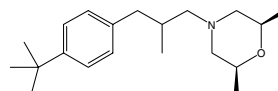
Cyclopropylmethyl-(1-ethyl-1,4-diphenyl-but-3-enyl)-methyl-amine

Haloperidol

4-[4-(4-Chlorophenyl)-4-hydroxy-1-piperidinyl-1'-(4-fluorophenyl)-1-butanone

DTG

1,3-Di-O-tolylguanidine

Fenpropimorph

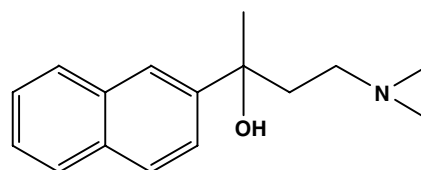
4-(3-(4-*tert*-butylphenyl)-2-methylpropyl)-2,6-dimethylmorpholine

Figure 1.

The σ_2 subtype of receptor, a 18–21 kDa protein, has not yet been cloned.¹² The binding profile of ligands for σ_2 receptors, unlike those for σ_1 , exhibits low affinities and no stereoselectivity for dextrorotatory benzomorphan. σ_2 receptor activation induces several biological effects including changes in cell morphology and apoptosis, and produces both transient and sustained increases in calcium ions.¹³ The important roles played by sigma receptors in certain biological systems suggest that the development of novel high-selective sigma ligands may provide potential drugs for CNS-related disorders and cancer diseases, since both sigma receptor subtypes are distributed within the central nervous system (particularly σ_1) and over-expressed in several tumor cell lines (particularly σ_2).^{5,7} σ_1 receptor neuromodulation could be the target of therapeutic strategies in many neurodegenerative diseases. For example, the relevant antidepressant efficacy of activators of σ_1 protein, especially progesterone, could be an effective approach to alleviate symptoms of depression in Alzheimer's disease.¹⁴ It has been pointed out that σ_1 selective agonists have potent anti-amnesic, antidepressant, and anti-stress effects, while selective antagonists have antipsychotic properties.¹⁵ σ_1 receptors are also involved in the modulation of opioid analgesia: (+)-pentazocine and 1,3-di(2-tolyl)guanidine (DTG) potently antagonize antinociceptivity, whereas σ_1 antagonists enhance opioid analgesia.^{16,17} For this reason, there is a growing interest in the potential clinical use of sigma ligands. Moreover, the discovery of selective

sigma ligands represents the only valid approach for characterizing sigma receptor subtypes better.

There are published reports on several highly selective σ_1 ligands synthesized to gain SAR information for a more detailed understanding of the pharmacological function of the σ_1 protein. In the last years molecular modeling studies have been performed to define the binding pharmacophore model for different classes of sigma ligands. Selective σ_1 pharmacophore models have been proposed by Glennon and Gund.^{18,19} Recently, results of our research on a series of naphthylalkylamines indicated that (*R/S*)-4-(dimethylamino)-2-(naphthalen-2-yl)butan-2-ol **1** (Fig. 2) is a ligand for σ_1 receptors. Compound **1** had been synthesized, together with some other compounds, to determine its possible involvement in opioid analgesia.²⁰ Pharmacological investigations using the hot plate test showed that this compound exerts antinociceptive properties and binding assays evidenced a significant affinity for σ_1 receptors ($K_i = 25$ nM).

**Figure 2.**

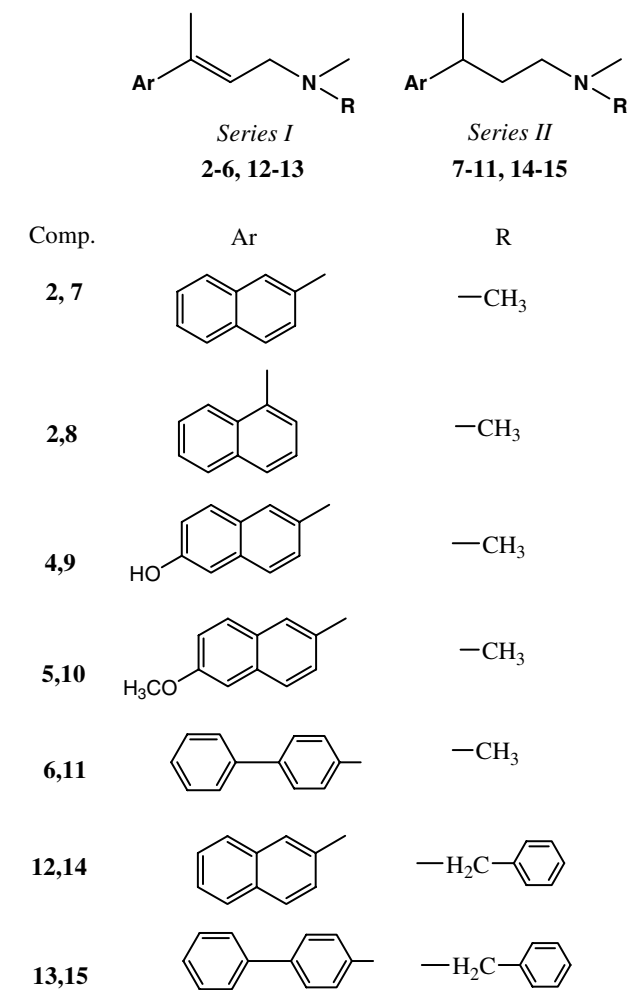


Figure 3.

On the basis of these encouraging results, in this paper, we report on the design, synthesis, and biological evaluation of new arylalkyl- and alkenylamines with different functionalities both on the aromatic moiety and the alkylamine chain (Fig. 3). We considered σ_1 selective pharmacophore models and investigated synthetic methods in order to prepare compounds with two independent points of diversity. SAR information on our novel σ_1 ligands was drawn on the basis of a new pharmacophore model developed by us.

2. Chemistry

2.1. Compounds' design

In order to develop σ_1 selective ligands, we selected (*R/S*)-4-(dimethylamino)-2-(naphthalen-2-yl)butan-2-ol **1** (Fig. 2) as the hit compound; we designed new analogues, using a computational approach and taking into account the selective σ_1 pharmacophore binding models proposed by Glennon and Gund.^{18,19}

The compounds were designed according to a conformational study that evaluated their degree of match with

the afore-mentioned pharmacophore models. The simpler model, proposed by Glennon et al., consisted of an amine-binding site flanked by a primary hydrophobic aromatic domain A and a secondary hydrophobic group B associated with a region of bulk tolerance.¹⁸ The more recent model by Gund complied with the topological arrangements of A, B, and N, but took into account an additional site corresponding to an electronegative atom such as oxygen or sulfur.¹⁹

A preliminary analysis of compound **1** was carried out with the aim of evaluating the possible role of oxygen in the σ_1 binding with respect to Gund's model. This conformational analysis was performed taking into account the physiological environment of the drug-receptor interaction (see Section 5.7). Despite the relatively high flexibility of the side chain of compound **1**, the distances between the alcoholic oxygen and the amino nitrogen as well as the aromatic centroid were not compatible with Gund's model in the most stable conformers (Fig. 4).

On the basis of these findings, we prepared the olefinic and saturated analogues **2–6** (Series I) and **7–11** (Series II) (Fig. 3) modifying both the aromatic nucleus and the 3-carbon dimethylamino side chain of the hit compound.

Moreover, the evaluation of structure–activity relationships of literature compounds suggested introducing a bulk substituent at the amino group.¹⁸ On the basis of these considerations, *N*-methyl-*N*-benzyl analogues of the most interesting compounds of both series were prepared, bearing the naphthalenic or the biphenylic moiety **12–13** (Series I) and **14–15** (Series II), in order to evaluate the influence of the amino substituent on the binding mode.

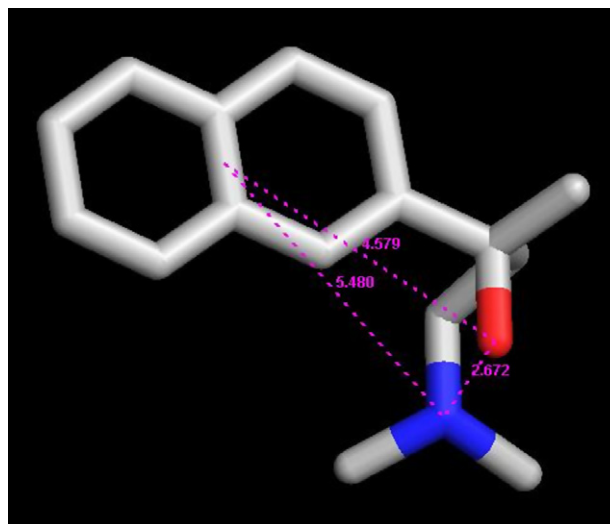


Figure 4. Global minimum conformer of **1** in polytube rendering. The distances reported in violet dashed lines were measured from the oxygen, the protonable nitrogen, and a dummy atom centered into the naphthalene ring. Hydrogen atoms were removed for clarity.

With regard to the drug-like properties, a preliminary evaluation of all the new derivatives was performed, considering the Lipinski's rule-of-five (molecular weight, H-bond donors, H-bond acceptors, and calculated log *P* values).²¹ The log *P* values of the examined compounds were calculated using the Daylight computational method (web version 4.91) that combines fragment lipophilicity contributions carefully parameterized with experimental data and calculated 'from scratch' values (Table 1).²² We had already validated this method for analogue compounds by comparison with chromatographic hydrophobicity values.²³ All the designed compounds were within the limits of Lipinski's rule-of-five with the exception of the compounds bearing an *N*-benzyl group. Despite this, compounds **12–15** were considered in the design strategy with the different purpose of testing the maximum length of the ligands that are able to fit into the σ_1 cleft. Therefore, we limited our evaluation to biphenyl and simple naphthalene aryl

derivatives, that is, without hydroxyl or methoxyl functions.

2.2. Synthesis

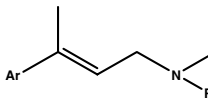
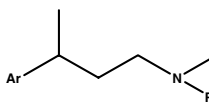
The general procedure for the preparation of the alkyl and alkenyl amines is reported in Scheme 1. We started our synthetic approach with the synthesis of β -aminoketones **16** and **17**, essentially prepared according to the convenient methodology described in our previous work, with suitable modifications (Scheme 2).²⁰ The Michael addition of the dimethylamine to but-3-en-2-one was performed in absolute ethanol and glacial acetic acid producing **16**, purified by fractional distillation. For compound **17**, benzyl-methyl-amine was employed and the reaction was performed in anhydrous toluene, thus producing the desired product in good yields, without any further purification. Thereafter, the compounds of Series I, **2–6** and **12–13**, were prepared by nucleophilic addition of the aromatic anion to β -aminoketones **16** and **17**, followed by direct dehydration in order to avoid isolation of the alcoholic intermediate (Scheme 2). An acid–base work-up allowed the isolation of the desired olefinic compounds with a good purity. In the case of compound **2**, quenching with HCl 37% led to the concurrent cleavage of the tetrahydropyranyl protecting group of the aromatic precursor 2-bromo-6-OTHP-naphthalene.

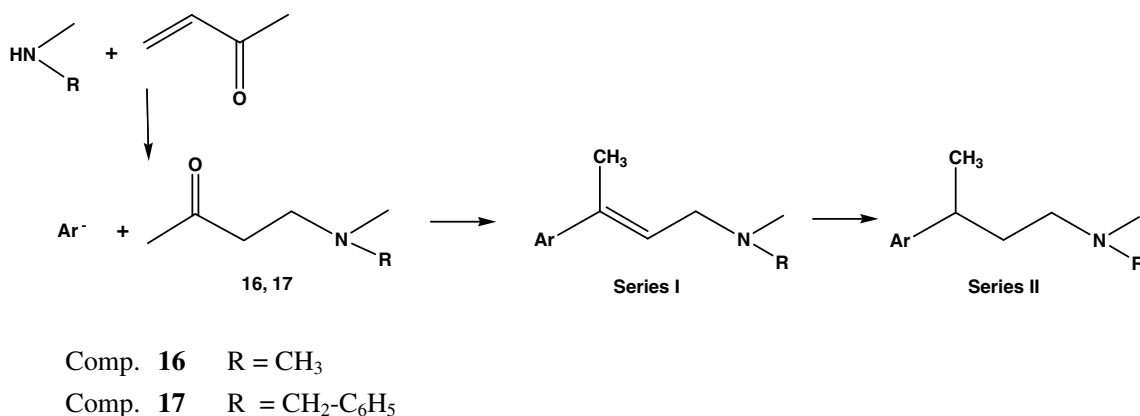
¹H NMR analyses of all crude compounds of Series I revealed the formation of a C2–C3 double bond and the absence of the signals related to C1–C2 olefinic regioisomers (Scheme 2); the ¹H NMR of compound **12** is reported in Figure 5 as an example. Regarding the configuration at the C2–C3 double bond, in all cases only one isomer was obtained (see Section 2.3). Actually, ¹H NMR analyses of compounds **2–6** and **12–13** showed only one signal corresponding to the olefinic proton; for the configurational assignment, see Section 2.3.

In conclusion, this procedure enabled easy generation of novel compounds at high purity.

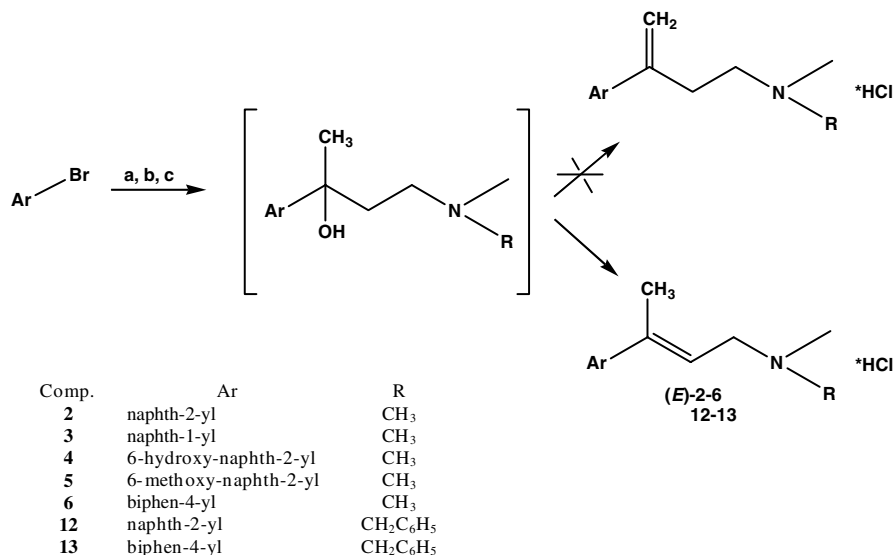
Series II compounds **7–11** were synthesized (Scheme 3) by catalytic reduction of the corresponding alkenes

Table 1.

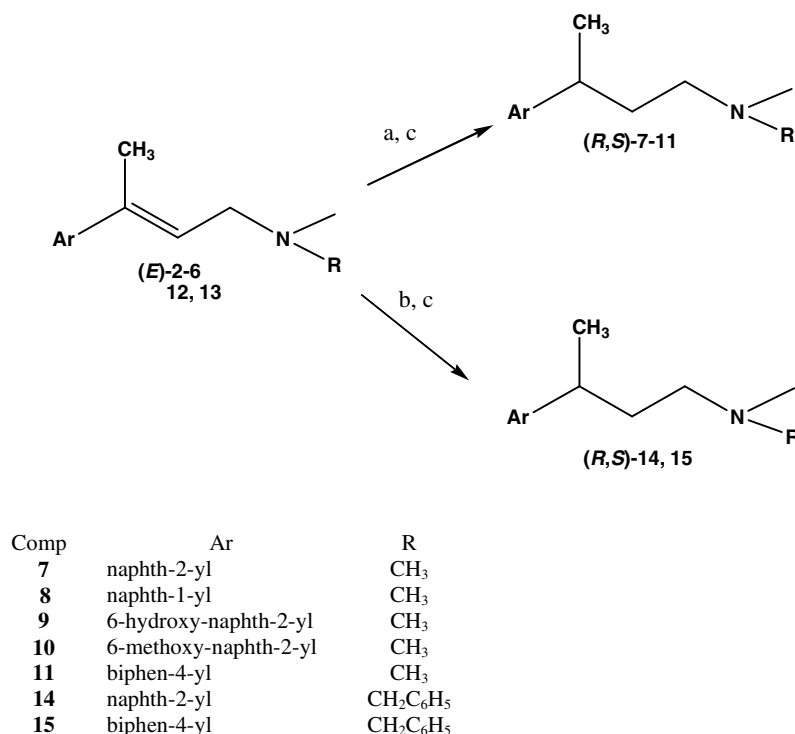
<div style="display: flex; justify-content: space-around; align-items: center;"> <div style="text-align: center;">  <p>(<i>E</i>)-2–6, 12–13 Series I</p> </div> <div style="text-align: center;">  <p>(<i>R/S</i>)-7–11, 14–15 Series II</p> </div> </div>			
Compound	Ar	R	Clog <i>P</i>
1	Naphth-2-yl	CH ₃	3.052
2	Naphth-2-yl	CH ₃	3.963
3	Naphth-1-yl	CH ₃	3.963
4	6-Hydroxy-naphth-2-yl	CH ₃	3.296
5	6-Methoxy-naphth-2-yl	CH ₃	3.882
6	Biphen-4-yl	CH ₃	4.677
7	Naphth-2-yl	CH ₃	4.067
8	Naphth-1-yl	CH ₃	4.067
9	6-Hydroxy-naphth-2-yl	CH ₃	3.400
10	6-Methoxy-naphth-2-yl	CH ₃	3.986
11	Biphen-4-yl	CH ₃	4.781
12	Naphth-2-yl	CH ₂ C ₆ H ₅	5.921
13	Biphen-4-yl	CH ₂ C ₆ H ₅	6.635
14	Naphth-2-yl	CH ₂ C ₆ H ₅	6.025
15	Biphen-4-yl	CH ₂ C ₆ H ₅	6.739



Scheme 1.



Scheme 2. Synthesis of (*E*)-4–8 and (*E*)-14–15. Reagents and conditions: (a) *t*-BuLi; (b) 2 or 3, anhydrous Et₂O, –78 °C; (c) HCl 37%, rt.



Scheme 3. Synthesis of (*R,S*)-9–13 and (*R,S*)-16–17. Reagents and conditions: (a) H₂, 10% Pd/C, CH₃OH, rt; (b) HCOONH₄, 10% Pd/C, absolute EtOH, rt; (c) HCOONH₄, EtOH, 10% Pd/C, 120°, 120 s.

2–6 with 10% Pd/C in a hydrogen atmosphere. Among the newly designed compounds, the alkylamines 14 and 15 could not be prepared using the above-described procedure. In fact, when 12 and 13 were reduced using conventional catalytic hydrogenation, concurrent cleavage of the *N*-benzyl group was observed.

The reaction was successful employing catalytic transfer hydrogenation (CTH) with ammonium formate as the hydrogen donor. Preliminary test runs with 2.5 equivalents of ammonium formate in the presence of 10%

Pd/C in methanol showed that the olefinic bond was completely reduced and cleavage of the *N*-benzyl group was avoided (Scheme 3). Compounds 14 and 15 were produced in this way, although long reaction times were required (12–24 h). It has recently been demonstrated that CTH can be conducted very rapidly and with good yields by employing microwave-assisted heating with a domestic microwave oven.²⁴ We, therefore, assayed the CTH procedure for all our compounds using a microwave oven specifically designed for organic synthesis (Discover LabMate single mode microwave, CEM Cor-

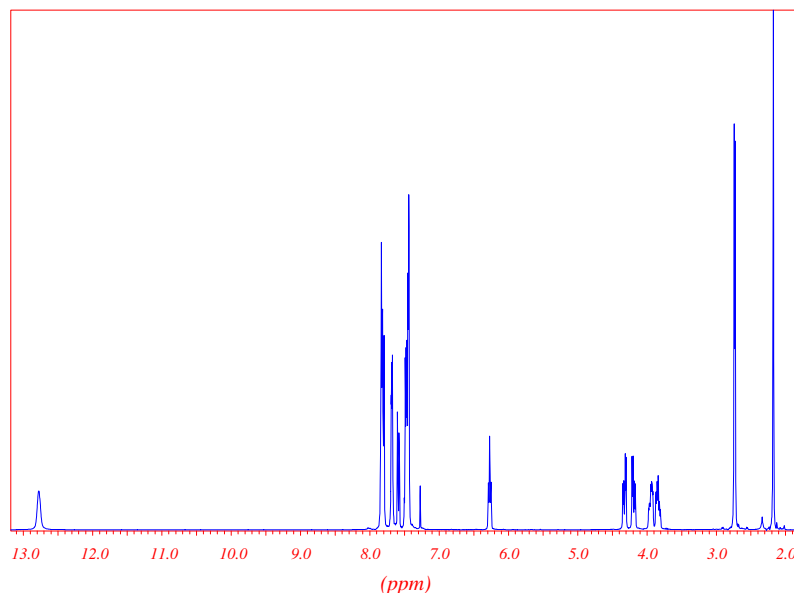


Figure 5. ^1H NMR spectrum of compound **12**.

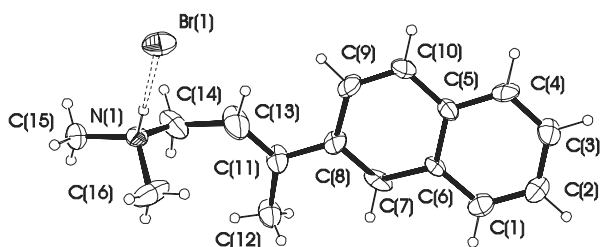


Figure 6. ORTEP drawing of **2** hydrobromide with the atom labeling scheme. Ellipsoids are drawn at the 30% probability level.

porate). This procedure was investigated varying the reaction times and the power. The best results were achieved with one step of irradiation at 140 °C for 90 s. Thus, all alkenes were rapidly reduced and the *N*-benzyl group of compounds **12–13** was not hydrogenolized.

2.3. Configurational study

In order to determine the stereochemistry of the olefinic bond, crystallographic analysis of **2** hydrobromide was performed together with 2D-NOESY NMR of all the compounds.

The structure of compound **2** was established by means of X-ray diffraction study. Single crystals suitable for the crystallographic analysis were obtained from slow crystallization (EtOH/H₂O) of the pure **2** hydrobromide. A stereoscopic view, with the atomic numbering scheme of the compound, obtained using the ORTEP 3 program, is shown in Figure 6.²⁵ Crystallographic data undoubtedly showed that the C=C bond is in the (*E*) configuration.

The NOESY analysis of compound **12** was compared with that of analogous **2**, bearing an *N,N*-dimethyl or an *N*-methyl-*N*-benzyl group, respectively. Both spectra

showed the presence of a significant NOE effect corresponding to the interaction of *h*, *l* and *h*, *m* protons (Fig. 7). Moreover, both *h* and *i* protons interact with the aromatic proton nucleus. No interactions were observed between *l* and *h*. These results are in agreement with the crystallographic analysis, confirming the (*E*) configuration also for compound **12**. On the basis of these findings, and taking into account the reaction mechanism, it is reasonable to attribute the *E* configuration to all compounds.

3. Results and discussion

3.1. In vitro binding assays

The binding properties of the novel compounds (Table 2) were investigated for sigma receptor subtypes (σ_1 and σ_2) expressed in guinea pig brain membranes. [³H]-(+)-pentazocine and [³H]DTG [1,3-di-2-tolylguanidine] were used as radioligands.

All new compounds **2–15** displayed interesting binding affinities for σ_1 subtype receptors (K_i values ranging from 1.02 to 47 nM, Table 2), with the exception of compounds **3** and **4**, confirming that the presence of the alcoholic group on the aliphatic chain of (*R/S*)-**1** is not essential for σ_1 affinity, according to the preliminary molecular modeling study (see Section 2.1).

First, we considered the new *N,N*-dimethylamino derivatives evaluating both the effects of the aromatic moiety and of the 3-carbon side chain on σ_1 affinity and σ_2/σ_1 selectivity.

The influence of the aromatic moiety on affinity (Table 2, Fig. 8) was particularly relevant for the compounds of Series I. Worse results were evidenced following replacement of the naphth-2-yl group (hit compound) with 6-hy-

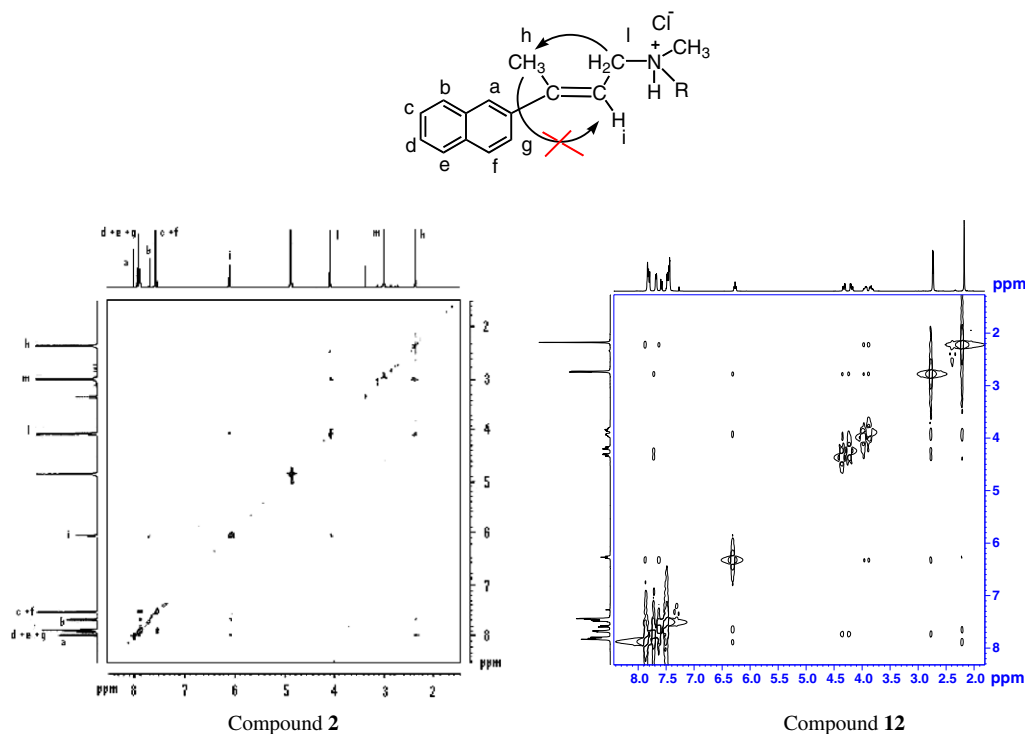


Figure 7. 2D ^1H ^1H NOESY of compounds **2** and **12**.

Table 2. Binding affinities of the synthesized compounds toward σ_1 and σ_2 receptors

Compound	Ar	R	K_i (nM) \pm SEM		
			σ_1^a	σ_2^b	σ_2/σ_1
1	Naphth-2-yl	CH ₃	25 \pm 0.4	171 \pm 5	6.8
2	Naphth-2-yl	CH ₃	19.8 \pm 0.3	148 \pm 4	7.5
3	Naphth-1-yl	CH ₃	102 \pm 5	701 \pm 21	6.87
4	6-Hydroxy-naphth-2-yl	CH ₃	229 \pm 3	1394 \pm 32	6.1
5	6-Methoxy-naphth-2-yl	CH ₃	21.4 \pm 0.8	985 \pm 16	46
6	Biphen-4-yl	CH ₃	1.40 \pm 0.2	106 \pm 6	75.7
7	Naphth-2-yl	CH ₃	1.95 \pm 0.2	43.8 \pm 3	22.5
8	Naphth-1-yl	CH ₃	47.2 \pm 1.0	205 \pm 5	4.3
9	6-Hydroxy-naphth-2-yl	CH ₃	19.0 \pm 0.8	1328 \pm 62	70
10	6-Methoxy-naphth-2-yl	CH ₃	2.30 \pm 0.2	60.4 \pm 7	26.3
11	Biphen-4-yl	CH ₃	1.02 \pm 0.2	161 \pm 5	157.8
12	Naphth-2-yl	CH ₂ C ₆ H ₅	7.88 \pm 0.3	873.1 \pm 12	110.8
13	Biphen-4-yl	CH ₂ C ₆ H ₅	6.32 \pm 0.3	75.7 \pm 4	12
14	Naphth-2-yl	CH ₂ C ₆ H ₅	5.4 \pm 0.3	139 \pm 4	25.7
15	Biphen-4-yl	CH ₂ C ₆ H ₅	5.8 \pm 0.4	591 \pm 25	102

Values are means \pm SEM of three experiments.

^a Displacement of 3 nM [^3H](+)-pentazocine.

^b Displacement of 3 nM [^3H]-DTG [1,3-di-(2-tolyl)-guanidine] in the presence of (+)-SKF10,047 (400 nM).

droxy-naphth-2-yl and naphth-1-yl. This was mainly evident for compound **4** (Series I) that showed a σ_1 affinity of 229 nM and only a 6-fold selectivity over σ_2 . Higher σ_1 receptor affinities ($K_i = 1.40$ and 1.02 nM) and better selectivities ($K_i\sigma_2/K_i\sigma_1 = 75.7$ and 157.8 , respectively) were evidenced for compounds **6** (Series I) and **11** (Series II), leading to the identification of the 4-biphenyl group as a promising aromatic moiety for both series.

As regards the effect of the 3-carbon dimethylamino side chain, binding data showed that Series II compounds had a better σ_1 affinity with respect to Series I (Table 2, Fig. 8).

Next, we investigated the influence of the aminic substituents on the binding mode by introducing a bulk substituent at the amino group, as suggested by the literature.¹⁸ We, therefore, prepared the *N*-methyl-*N*-benzyl analogues of the most interesting compounds of both series, bearing the 2-naphthalenic or the 4-biphenylic moiety. In contrast to our hypothesis, the presence of the *N*-benzyl group increased both σ_1 affinity and selectivity in the naphth-2-yl derivatives **12** and **14** only. In fact, the introduction of an *N*-benzyl group in the 4-biphenyl derivatives lowered both σ_1 affinity and selectivity. Moreover, all *N*-benzylamino derivatives showed remarkable affinity for σ_1 (K_i nM ranging from 5.4 to

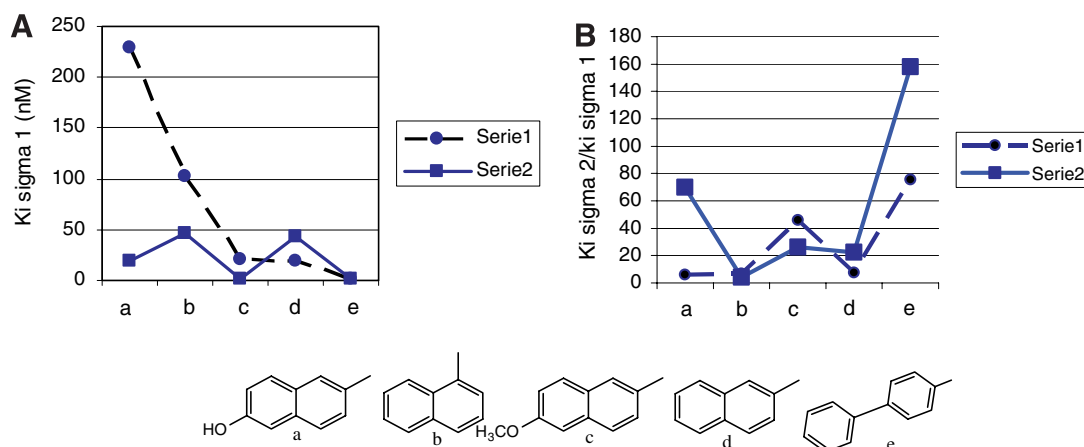


Figure 8. Effects of the aromatic substituents on σ_1 affinity (A) and on σ_1/σ_2 selectivity (B) of *N,N*-dimethylamino derivatives.

7.9 nM), but only compound **12** also showed a good selectivity (110.8).

These results indicate that the best influence on σ_1 affinity and selectivity is related to the presence of the 4-biphenyl moiety. In contrast, the introduction of a benzyl group at the amine site is not always a convenient modification. On the basis of these findings, it can be postulated that when the sigma ligands possess two aromatic moieties, the balance between their steric hindrances is particularly relevant for the binding.

3.2. Molecular modeling

The compound design allowed us to obtain novel interesting σ_1 ligands, even though neither of the pharmacophore models considered was able to explain some of the structure–activity relationships.

To gain more insights into binding modes and to perform a more rational SAR study, we mapped conformers of the synthesized compounds onto a 5-point pharmacophore model developed by us using the Hypo-Gen module in Catalyst 4.9 and which we have de-

scribed in detail in a previous paper where it has also been successfully used to find novel screening candidates.^{26,27} This model consisted of four hydrophobic and one positive ionizable features. Our own model²⁷ was in good agreement with the model proposed by Glennon, which was not a computational model and therefore not fit for in silico comparison with compound models and for database screening. Our model did not possess the additional electronegative site reported by Gund either. This additional feature is present in many known σ_1 -active compounds, but does not seem to be important for affinity toward this target. Since most of our compounds also lacked this feature, our own model seemed to be better suited for predicting their binding modes. A short overview of the three models is given in Table 3.

This model was able to fit all our molecules, although their affinities were always overestimated by factors ranging from 2 to 4900. Such an overestimation may be attributed to both interlaboratory differences—the training set for the Catalyst model and the compounds presented in this paper were tested in different laboratories—and also to the very high σ_1 affinity ($K_i = 0.01$ nM)

Table 3. Comparison of previously reported σ_1 models including our own model

Reference	Glennon et al. ¹⁸	Gund et al. ¹⁹	Laggner et al. ²⁷
Data used for model generation	SAR of 49 compounds	Guided overlay of low-energy conformations of four compounds	Automatic overlay of conformational models from 23 compounds, inclusion of binding-affinity data (QSAR model)
Software package used	Is not an in silico model	Sybyl 6.5	Catalyst 4.9
Distance between basic site and primary hydrophobic site (Å)	6–10	7.14	Two features at 6.3 and 9.8 Å, respectively
Distance between basic site and secondary hydrophobic site (Å)	2.5–3.9	2.80	4.1
Additional interaction sites	None	Hydrogen-bond accepting feature in direction of primary hydrophobic group, 4.17 Å from basic site	Fourth hydrophobic region in direction of primary hydrophobic group, 3.6 Å from basic site
Additional restrictions	Basic site ('proton donor site') tolerates small groups only, secondary binding site tolerates bulk	Aromatic rings at the primary hydrophobic feature lie inside a plane—two additional points for orientation	For database searching (not used in this paper): predicted K_i value <100 μ M, molecular weight <600, and inclusion of molecular shape of fenpropimorph

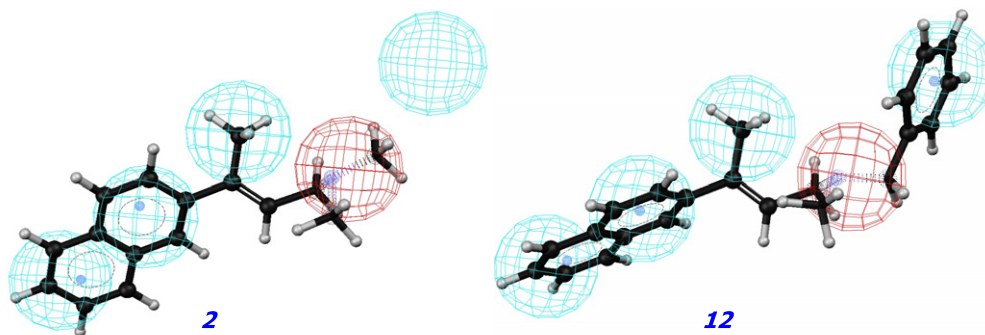


Figure 9. Mapping of compounds **2** and **12** onto our σ_1 pharmacophore model: positive ionizable feature, red sphere; hydrophobic features, cyan spheres.

of fenpropimorph (Fig. 1) in the training set of selected compounds, which tuned the model toward high affinity values. It should be pointed out that this compound is very similar to our own compounds, both consisting of an aromatic ring connected to a tertiary amine through a chain of three carbon atoms. Methyl groups of the side chain at the α and β positions of fenpropimorph and of our compounds are able to map the same pharmacophore feature. Additionally, the second phenyl group in our biphenyl derivatives may play a similar role to that of the *tert*-butyl group of fenpropimorph.

Because of the observed overestimation, instead of considering the absolute K_i values we compared best fit values ranging from 0 to 10.7, the latter value describing the perfect fit of **14**.

According to the SAR study, removal of the alcoholic group from **1** resulted in a better fitting of **2** and **7** (best fit values: 8.19 and 8.46 vs 6.44). The replacement of the *N,N*-dimethyl group by an *N*-methyl-*N*-benzyl group was expected to be advantageous since the *N*-benzyl derivatives were associated with the highest best fit values (e.g., **12** showed the highest value of 10.7, whereas its *N,N*-dimethyl analogue **2** had a value of 8.19) (Fig. 9).

Interestingly, 1-naphthyl substitution was also predicted to have negative effects since **3** and **8**, not being able to map the hydrophobic site furthest away from the positive ionizable center, showed values of 6.51 and 6.54, respectively, whereas the 2-naphthyl derivatives **2** and **7** that failed only to map the hydrophobic site closest to the amino group showed fit values of 8.19 and 8.46.

However, the influence of the 4-biphenyl substitution was not correctly predicted by our Catalyst pharmacophore model, according to which the effects of the benzyl group at the amine site were always the most important. For example, our model was not able to explain the significantly enhanced activity for *N,N*-dimethyl substituted 4-biphenyl derivatives **6** and **11**, for which it predicted slightly worse affinities than for their naphthyl analogues **2** and **7**. In good accordance with the binding data, comparable best fit values were found for **6** and **11** (8.05 vs 8.35), so far identified as the most active compounds of our series.

Fitting studies for both isomers of all synthesized alkenes (**2–6** and **12**, **13**) indicated that (*E*)-alkenes, which were the sole products retrieved under our reaction conditions, should be much more active than their (*Z*)-counterparts. (*E*)-**13** showed a significantly better fit than its (*Z*)-isomer (best fit values: 10.17 vs 8.35), whereas very small differences were found between the two stereoisomers of **5** and **6** (difference between the best fit values: 0.54, 0.05).

The role of the stereochemistry in binding requirements was further investigated extending fitting studies to the pure enantiomeric (*R*) and (*S*) forms of alkanes **7–11** and **14**, **15**. With the exception of **8** and **10**, (*S*) isomers were predicted to be slightly more active than the (*R*) isomers. Only slight differences were found for each pair of enantiomers: the highest difference in fit values was 0.7 for the enantiomers of **7**.

In the future, pure enantiomers of the most interesting saturated ligands will be prepared in order to assess our model's prediction about the relationship between stereochemistry at the benzylic carbon atom and the receptor binding affinity.

4. Conclusion

We present the design, synthesis, and biological evaluation of a novel class of arylalkyl- and alkenylamines, new molecules with novel structures, strong affinities, and high selectivity.

The application of indirect modeling approaches involving the analysis of known pharmacophore models allowed us to design novel σ_1 ligands efficiently. The starting point of our study was (*R/S*)-4-(dimethylamino)-2-(naphthalene-2-yl)butan-2-ol **1**, previously synthesized in our laboratory and characterized by promising affinity for σ_1 receptors. Racemic *N,N*-dimethyl-3-(6-hydroxynaphthalen-2-yl)butan-1-amine **11** showed not only potent affinity for σ_1 receptor, but good selectivity over the σ_2 subtype.

Moreover, useful information concerning the structure and properties of the ligand-binding site in the σ_1 receptor was obtained. Evaluation of the degree of fit between all

the new ligands and a five-point pharmacophore model, developed using the HypoGen module within the software package Catalyst,²⁷ allowed us to acquire more insights to improve this model and to establish more coherent structure–activity relationships. Despite some weaknesses in quantitative predictions, this pharmacophore model never produced false-negative results and consequently encourages us to use it for the design and synthesis of more potent and selective σ_1 ligands. With this aim, the model will be used for virtual screening of libraries of potential novel ligands, based on the structures of the most active and selective compounds so far identified.

Our aim for the future is to prepare and test the pure enantiomers of the most active and selective compounds but also perform functional assays studying the interaction with some neuroactive steroids. The results of such investigations will allow us to evaluate both their agonistic/antagonistic activity.

5. Experimental

5.1. General methods

Unless otherwise specified, commercially available reagents and solvents were used as received from the supplier. Anhydrous solvents were obtained according to standard procedures.

Melting points were measured on SMP3 Stuart Scientific apparatus and are uncorrected. Elemental analyses were performed on a Carlo Erba 1106 C, H, N analyzer.

Analytical TLC were carried out on silica gel pre-coated glass-backed plates (Fluka Kieselgel 60 F₂₅₄, Merck) and visualized by ultra-violet radiation, acidic ammonium molybdate (IV) or potassium permanganate.

X-ray crystallographic analysis was performed on Philips Pw 1100 computer-controlled four circle diffractometer, graphite-monochromated MoK α radiation, ω scan technique ($\pm h$, $\pm k$, and $\pm l$), scan width 1.5°, scan speed 0.05°/min, range 2–20° theta. IR spectra were recorded on a Jasco FT/IR-4100 spectrophotometer; only noteworthy absorptions are given. ¹H NMR spectra were measured with an ADVANCE 400 spectrometer Bruker, Germany; TMS was used as internal standard $\delta = 0$ and chemical shifts are given in ppm.

Microwave dielectric heating was performed in a Discover[®] LabMate instrument, CEM Corporate specifically designed for organic synthesis and following an appropriate microwave program. The reaction temperatures were monitored by an IR probe.

5.2. 4-(Benzyl-methyl-amino)butan-2-one (17)

Methylvinylketone (12 mL, 146 mmol) was added dropwise to a stirred solution of *N*-benzyl-*N*-methyl-amine (13 mL, 102.2 mmol) in anhydrous toluene (1 M). The reaction mixture was refluxed for 4 h under a nitrogen

atmosphere and then HCl 1 N was added until pH 2 was reached. The aqueous phase was washed with diethyl ether, made alkaline with a saturated solution of NaHCO₃ to pH 8, and extracted with CHCl₃. The combined organic layers were dried over anhydrous Na₂SO₄ and concentrated under reduced pressure yielding the desired product as a yellow oil. The yield was 83%. IR (cm⁻¹): 3025, 2946, 1710, 1600, 1494, 1455, 1355, 1163, 1025, 916, 749. ¹H NMR (CDCl₃) δ 2.16 (s, 3H, CH₃–CO), 2.21 (s, 3H, CH₃–N), 2.70 (dt, 4H, CH₂–CH₂–N, *J* = 6.4 Hz), 3.52 (s, 2H, CH₂–C₆H₅), 7.31 (m, 5H, aromatic). Elemental analysis calculated for C₁₂H₁₇NO: C, 75.35; H, 8.96; N, 7.32. Found: C, 75.16; H, 8.88; N, 7.54.

5.3. General procedure for the preparation of compounds (E)-2–8 hydrochlorides

t-BuLi (17.16 mmol, 1.7 M in pentane) was added dropwise to a solution of the corresponding aromatic precursor (8.58 mmol) in anhydrous diethyl ether (0.2 M) cooled to –78 °C, under nitrogen atmosphere, keeping the temperature for 15 min. The reaction mixture was then allowed to warm slowly to room temperature. Stirring was continued for 1 h and a solution of the ketone (6.86 mmol) in dry diethyl ether (10 mL) at –78 °C was then added dropwise. After 2 h, the reaction mixture was quenched with HCl 10 N until pH 2. The precipitate obtained was filtered off and, after an acid–base work-up, was crystallized from acetone providing the expected product as a white solid.

5.3.1. (E)-*N,N*-Dimethyl-3-(naphthalen-2-yl)but-2-en-1-yl-amine hydrochloride [(E)-2-HCl]. Yield 76%; white solid, mp 201–203 °C. IR (cm⁻¹): 3051, 2892, 2563, 2477, 2366, 2310, 1632, 1475, 1384, 1130, 950, 820, 741. ¹H NMR (CD₃OD) δ 2.30 (s, 3H, CH₃C=CH), 2.94 (s, 6H, N(CH₃)₂), 4.03 (d, 2H, CH₂–N, *J* = 7.8 Hz), 6.02 (t, 1H, CH₃C=CH, *J* = 7.8 Hz), 7.48 (m, 2H, aromatic), 7.64 (d, 1H, aromatic, *J* = 7.8 Hz), 7.80 (m, 3H, aromatic), 7.95 (s, 1H, aromatic). Elemental analysis calculated for C₁₆H₂₀NCl: C, 73.41; H, 7.70; N, 5.35. Found: C, 73.14; H, 7.57; N, 5.16.

5.3.2. (E)-*N,N*-Dimethyl-3-(naphthalen-1-yl)but-2-en-1-yl-amine hydrochloride [(E)-3-HCl]. Yield 59%; white solid, mp 192–194 °C. IR (cm⁻¹): 3011, 2899, 2617, 2361, 1656, 1460, 1376, 1161, 1010, 777. ¹H NMR (CD₃OD) δ 2.27 (s, 3H, CH₃C=CH), 3.32 (s, 6H, N(CH₃)₂), 4.05 (d, 2H, CH₂–N, *J* = 8.3 Hz), 5.65 (dt, 1H, CH₃C=CH, *J* = 7.8 Hz), 7.34 (dd, 1H, aromatic, *J* = 6.9 Hz), 7.47 (d, 1H, aromatic, *J* = 8.3 Hz), 7.52 (m, 2H, aromatic), 7.90 (m, 3H, aromatic). Elemental analysis calculated for C₁₆H₂₀NCl: C, 73.41; H, 7.70; N, 5.35. Found: C, 73.30; H, 7.68; N, 5.44.

5.3.3. (E)-*N,N*-Dimethyl-3-(6-hydroxy-naphthalen-2-yl)but-2-en-1-yl-amine hydrochloride [(E)-4-HCl]. Yield 38%; white solid, mp 219–220 °C. IR (cm⁻¹): 3200, 2700, 2640, 2510, 1630, 1425, 1260, 1150, 950, 860. ¹H NMR (CD₃OD) δ 2.38 (s, 3H, CH₃C=CH), 3.0 (s, 6H, N(CH₃)₂), 4.11 (d, 2H, CH₂–N, *J* = 7.8 Hz), 6.06 (t, 1H, CH₃C=CH, *J* = 7.7 Hz), 7.16 (d, 1H, aromatic,

$J = 2.4$ Hz), 7.19 (s, 1H, aromatic), 7.65 (d, 1H, aromatic, $J = 8.7$ Hz), 7.73 (d, 1H, aromatic, $J = 8.7$ Hz), 7.84 (d, 1H, aromatic, $J = 8.5$ Hz), 7.95 (s, 1H, aromatic). Elemental analysis calculated for $C_{16}H_{20}NOCl$: C, 69.18; H, 7.26; N, 5.04. Found: C, 68.79; H, 7.54; N, 4.92.

5.3.4. (*E*)-*N,N*-Dimethyl-3-(6-methoxy-naphthalen-2-yl)but-2-en-1-yl-amine hydrochloride [(*E*)-5-HCl]. Yield 70%; white solid, mp 240–241 °C. IR (cm^{-1}): 3008, 2938, 2589, 2485, 2350, 1598, 1482, 1246, 1028, 851. 1H NMR (CD_3OD) δ 2.17 (s, 3H, $CH_3C=CH$), 2.76 (s, 6H, $N(CH_3)_2$), 3.80 (m, 5H, $CH_2-N + OCH_3$), 5.87 (t, 1H, $CH_3C=CH$, $J = 7.8$ Hz), 7.03 (dd, 1H, aromatic, $J = 8.8$ Hz), 7.12 (s, 1H, aromatic), 7.50 (dd, 1H, aromatic, $J = 8.8$ Hz), 7.66 (m, 2H, aromatic), 7.76 (s, 1H, aromatic). Elemental analysis calculated for $C_{17}H_{22}NOCl$: C, 69.97; H, 7.70; N, 4.80. Found: C, 69.87; H, 7.64; N, 4.45.

5.3.5. (*E*)-*N,N*-Dimethyl-3-(biphen-4-yl)but-2-en-1-yl-amine hydrochloride [(*E*)-6-HCl]. Yield 63%; white solid, mp 251–252 °C. IR (cm^{-1}): 3007, 2950, 2569, 2513, 2478, 2376, 1642, 1485, 1300, 952, 841, 758. 1H NMR (CD_3OD) δ 2.13 (s, 3H, $CH_3C=CH$), 2.87 (s, 6H, $N(CH_3)_2$), 3.89 (d, 2H, CH_2-N , $J = 7.8$ Hz), 5.83 (dt, 1H, $CH_3C=CH$, $J = 7.3$ Hz), 7.22 (dt, 1H, aromatic, $J = 7.3$ Hz), 7.33 (dt, 2H, aromatic, $J = 7.3$ Hz), 7.48 (dd, 2H, aromatic, $J = 8.8$ Hz), 7.52 (m, 4H, aromatic). Elemental analysis calculated for $C_{18}H_{22}NCl$: C, 75.11; H, 7.70; N, 4.87. Found: C, 75.22; H, 7.94; N, 5.03.

5.3.6. (*E*)-*N*-Benzyl-*N*-methyl-3-(naphthalen-2-yl)but-2-en-1-yl-amine hydrochloride [(*E*)-7-HCl]. Yield 43%; white solid, mp 179–180 °C. IR (cm^{-1}): 3049, 2969, 2585, 2514, 1647, 1472, 1444, 1389, 906, 818, 745. 1H NMR (CD_3OD) δ 2.29 (s, 3H, $CH_3C=CH$), 2.88 (s, 3H, $N-CH_3$), 4.09 (d, 2H, CH_2-N , $J = 7.8$ Hz), 4.45 (s, 2H, $CH_2-C_6H_5$), 6.08 (dt, 1H, $CH_3C=CH$, $J = 7.8$ Hz), 7.55 (m, 7H, aromatic), 7.67 (dd, 1H, aromatic, $J = 8.8$ Hz), 7.88 (m, 3H, aromatic), 7.97 (s, 1H, aromatic). Elemental analysis calculated for $C_{22}H_{24}NCl$: C, 78.20; H, 7.16; N, 4.15. Found: C, 77.81; H, 7.40; N, 4.40.

5.3.7. (*E*)-*N*-Benzyl-*N*-methyl-3-(biphen-4-yl)but-2-en-1-yl-amine hydrochloride [(*E*)-8-HCl]. Yield 27%; white solid, mp 223–224 °C. IR (cm^{-1}): 3030, 2979, 2487, 2381, 1644, 1468, 1420, 1375, 1100, 1054, 918, 765. 1H NMR (CD_3OD) δ 2.08 (s, 3H, $CH_3C=CH$), 2.73 (s, 3H, $N-CH_3$), 3.93 (d, 2H, CH_2-N , $J = 7.6$ Hz), 4.30 (s, 2H, $CH_2-C_6H_5$), 5.87 (dt, 1H, $CH_3C=CH$, $J = 7.8$ Hz), 7.23 (t, 1H, aromatic, $J = 7.3$ Hz), 7.33 (dt, 2H, aromatic, $J = 7.3$ Hz), 7.42 (m, 6H, aromatic), 7.48 (s, 1H, aromatic), 7.52 (m, 4H, aromatic). Elemental analysis calculated for $C_{24}H_{26}NCl$: C, 79.21; H, 7.20; N, 3.85. Found: C, 79.36; H, 7.38; N, 3.74.

5.4. General procedure for the preparation of (*R/S*)-7-11 and (*R/S*)-14-15 hydrochlorides

5.4.1. Method A. 10% Pd/C (0.044 mmol) was added to a stirred solution of the corresponding alkenes (*E*)-2–

6-HCl (4.44 mmol) in methanol (0.1 M, 44.4 mL) in a hydrogen atmosphere. After 24 h, the reaction mixture was filtered on a pad of Celite and washed thoroughly with methanol. After evaporation of the solvent under vacuum, the crude product was crystallized from acetone giving the desired compound as a white solid.

5.4.2. Method B. 10% Pd/C (0.33 g) and ammonium formate (8.31 mmol) were added to a stirred solution of the corresponding alkenes (*E*)-12–13 (3.32 mmol) in absolute ethanol (28 mL). After 6 h, the reaction mixture was filtered on a pad of Celite and washed thoroughly with absolute ethanol. After an acid–base work-up, the reaction solvent was evaporated under vacuum and the crude product was transformed into the corresponding hydrochloride and crystallized from acetone providing the product as a white solid.

5.4.3. Method C. Ammonium formate (0.75 mmol) and 10% Pd/C (30 mg) were added to alkenes (*E*)-2–6, 12–13 (0.3 mmol) in absolute ethanol (3 mL) placed in a MW vial. The mixture was heated for 90 s at 100 W. After the usual work-up, the desired products were isolated.

5.4.4. (*R/S*)-*N,N*-Dimethyl-3-(naphthalen-2-yl)butan-1-amine hydrochloride [(*R/S*)-9-HCl]. Yield 59%; white solid, mp 177–179 °C. IR (cm^{-1}): 3362, 3010, 2776, 2577, 2467, 1599, 1474, 1190, 1014, 963, 751. 1H NMR (CD_3OD) δ 1.35 (d, 3H, CH_3-CH , $J = 7.1$ Hz), 1.89 (m, 2H, $CH-CH_2$), 2.18 (s, 6H, $N(CH_3)_2$), 2.30 (m, 2H, CH_2-N), 2.87 (m, 1H, CH_3-CH), 7.4 (m, 3H, aromatic), 7.63 (s, 1H, aromatic), 7.80 (m, 3H, aromatic). Elemental analysis calculated for $C_{16}H_{22}NCl$: C, 72.85; H, 8.41; N, 5.31. Found: C, 73.01; H, 8.33; N, 5.32.

5.4.5. (*R/S*)-*N,N*-Dimethyl-3-(naphthalen-1-yl)butan-1-amine hydrochloride [(*R/S*)-10-HCl]. Yield 32%; white solid, mp 195–199 °C. IR (cm^{-1}): 3371, 3015, 2873, 2577, 2477, 1593, 1479, 1396, 964, 803, 780. 1H NMR (CD_3OD) δ 1.38 (d, 3H, CH_3-CH , $J = 7.3$ Hz), 2.16 (m, 2H, $CH-CH_2$), 2.75 (s, 6H, $N(CH_3)_2$), 2.92 (dt, 1H, $HCH-N$, $J = 5.4$, 12.2 Hz), 3.09 (dt, 1H, $HCH-N$, $J = 5.4$, 12.2 Hz), 3.72 (m, 1H, CH_3-CH), 7.43 (m, 3H, aromatic), 7.48 (dt, 1H, aromatic, $J = 6.9$ Hz), 7.69 (dd, 1H, aromatic, $J = 6.4$ Hz), 7.81 (d, 1H, aromatic, $J = 7.8$ Hz), 8.1 (d, 1H, aromatic, $J = 8.3$ Hz). Elemental analysis calculated for $C_{16}H_{22}NCl$: C, 72.85; H, 8.41; N, 5.31. Found: C, 72.60; H, 8.65; N, 5.34.

5.4.6. (*R/S*)-*N,N*-Dimethyl-3-(6-hydroxy-naphthalen-2-yl)butan-1-amine hydrochloride [(*R/S*)-11-HCl]. Yield 69%; white solid, mp 165–167 °C. IR (cm^{-1}): 3211, 2706, 2575, 2475, 1602, 1476, 1387, 1363, 1185, 853. 1H NMR (CD_3OD) δ 1.30 (d, 3H, CH_3-CH , $J = 6.6$ Hz), 2.03 (m, 2H, $CH-CH_2$), 2.72 (s, 6H, $N(CH_3)_2$), 2.83 (m, 2H, CH_2-N), 3.01 (m, 1H, CH_3-CH), 7.0 (sb+d, 2H, aromatic, $J = 9.8$ Hz), 7.24 (d, 1H, aromatic, $J = 8.4$ Hz), 7.5 (s, 1H, aromatic), 7.55 (d, 1H, aromatic, $J = 8.5$ Hz), 7.59 (d, 1H, aromatic, $J = 8.7$ Hz). Elemental analysis calculated for $C_{16}H_{22}NOCl$: C, 68.68; H, 7.93; N, 5.01. Found: C, 69.07; H, 8.09; N, 4.88.

5.4.7. (*R/S*)-*N,N*-Dimethyl-3-(6-methoxy-naphthalen-2-yl) butan-1-amine hydrochloride [(*R/S*)-12·HCl]. Yield 53%; white solid, mp 217–224 °C. IR (cm⁻¹): 3398, 2957, 2597, 2518, 2485, 1604, 1482, 1217, 1024, 849. ¹H NMR (CD₃OD) δ 1.39 (d, 3H, CH₃–CH, *J* = 6.7 Hz), 2.09 (m, 2H, CH–CH₂), 2.80 (s, 6H, N(CH₃)₂), 2.92 (m, 2H, CH₂–N), 3.12 (m, 1H, CH₃–CH), 3.88 (s, 3H, OCH₃), 7.10 (dd, 1H, aromatic, *J* = 8.8 Hz), 7.19 (s, 1H, aromatic), 7.36 (d, 1H, aromatic, *J* = 8.8 Hz), 7.60 (s, 1H, aromatic), 7.69 (d, 1H, aromatic, *J* = 8.4 Hz), 7.75 (d, 1H, aromatic, *J* = 8.4 Hz). Elemental analysis calculated for C₁₇H₂₄NOCl: C, 69.49; H, 8.23; N, 4.77. Found: C, 69.87; H, 8.56; N, 4.94.

5.4.8. (*R/S*)-*N,N*-Dimethyl-3-(biphen-4-yl)butan-1-amine hydrochloride [(*R/S*)-13·HCl]. Yield 47%, white solid, mp 203–204 °C. IR (cm⁻¹): 3051, 2881, 2550, 2469, 2408, 1600, 1485, 1406, 1006, 966, 835. ¹H NMR (CD₃OD) δ 1.38 (d, 3H, CH₃–CH, *J* = 6.9 Hz), 2.07 (m, 2H, CH–CH₂), 2.85 (s, 6H, N(CH₃)₂), 2.88 (m, 2H, CH₂–N), 3.15 (m, 1H, CH₃–CH), 7.35 (m, 3H, aromatic), 7.44 (t, 2H, aromatic, *J* = 8.3 Hz), 7.60 (m, 4H, aromatic). Elemental analysis calculated for C₁₈H₂₄NCl: C, 74.59; H, 8.35; N, 4.83. Found: C, 74.41; H, 8.35; N, 4.45.

5.4.9. (*R/S*)-*N*-Benzyl-*N*-methyl-3-(naphthalen-2-yl)butan-1-amine hydrochloride [(*R/S*)-14·HCl]. Yield 25%, white solid, mp 143–144 °C. IR (cm⁻¹): 3033, 2526, 2348, 1867, 1747, 1650, 1396, 1147, 1027, 818, 748. ¹H NMR (CDCl₃) δ 1.44 (d, 3H, CH₃–CH, *J* = 6.8 Hz), 2.20 (m, 2H, CH–CH₂), 2.78 (s, 3H, N–CH₃), 2.98 (m, 1H, HCH–N), 3.16 (m, 1H, HCH–N), 4.25 (m, 1H, CH₃–CH), 4.26 (s, 2H, CH₂–C₆H₅), 7.36 (m, 6H, aromatic), 7.48 (m, 2H, aromatic), 7.67 (s, 1H, aromatic), 7.83 (m, 3H, aromatic). Elemental analysis calculated for C₂₂H₂₆NCl: C, 77.74; H, 7.71; N, 4.12. Found: C, 77.37; H, 8.04; N, 4.01.

5.4.10. (*R/S*)-*N*-Benzyl-*N*-methyl-3-(biphen-4-yl)butan-1-amine hydrochloride [(*R/S*)-15·HCl]. Yield 15%, white solid, mp 144–146 °C. IR (cm⁻¹): 3054, 2849, 2566, 2502, 1670, 1484, 1454, 1074, 835, 763. ¹H NMR (CDCl₃) δ 1.28 (d, 3H, CH₃–CH, *J* = 7.8 Hz), 1.85 (m, 2H, CH–CH₂), 2.17 (s, 3H, N–CH₃), 2.35 (m, 2H, CH₂–N), 2.85 (m, 1H, CH₃–CH), 3.46 (s, 2H, CH₂–C₆H₅), 7.29 (m, 8H, aromatic), 7.44 (t, 2H, aromatic, *J* = 7.6 Hz), 7.52 (d, 2H, aromatic, *J* = 8.1 Hz), 7.60 (d, 2H, aromatic, *J* = 7.3 Hz). Elemental analysis calculated for C₂₄H₂₈NCl: C, 78.77; H, 7.71; N, 3.83. Found: C, 78.74; H, 7.79; N, 3.81.

5.5. Crystal data for C₁₆H₂₀ NBr 2

Monocyclic, space group *P*₂₁/*c*, *a* = 20.922(5) Å, *b* = 5.5923(11) Å, *c* = 12.634(2) Å, β = 93.141 (18)°, *V* = 1476.0(5) Å³, *Z* = 4, *d*_x = 1.378 g cm⁻³, *T* = 293 K. Data were collected for a colorless needle-shaped crystal with dimensions of 0.12 mm × 0.15 mm × 0.30 mm on a Philips Pw 1100 computer-controlled four circle diffractometer, graphite-monochromated MoKα radiation. Final *R* indices for 770 reflections with *I* > 2σ (*I*) and 169

refined parameters are the following: *R*₁ = 0.0589, *wR*₂ = 0.1007 (*R*₁ = 0.1292, *wR*₂ = 0.1219 for all 1382 data). Atomic coordinates and anisotropic displacement parameters are for deposit.

5.6. ¹H NMR spectroscopy

¹H, ¹H COSY, and 2D-NOESY NMR spectra of *E*-2 and *E*-12 were performed at 9.4 T, in CD₃OD at room temperature (TMS as internal standard δ = 0).

5.7. Molecular modeling

5.7.1. Conformational search of compound 1. Compound 1 was built by the Maestro user interface of MACRO-MODEL ver 7.2.²⁸ Energy was minimized with the MMFFs force field²⁸ and GB/SA implicit model of solvation.²⁹ As previously reported in a similar compound analysis, the nitrogen atom was considered to be in protonated form.³⁰ The automatic setup included five torsional bonds. A Monte Carlo (MC) search³¹ was used to generate 2000 conformations and energy was minimized with the same force field and solvation conditions. The deduplication of identical conformers after superimposition was performed according to the standard MACROMODEL criteria (max rms deviation equal to 0.25 Å, max energy difference equal to 1 kcal/mol).

The pharmacophore feature measurements were carried out with the Maestro graphical interface considering for the aromatic moiety the centroid averaging the position of the naphthalene carbon atoms, for the protonated amine the nitrogen atom, and for the hydroxyl moiety the oxygen atom. All calculations were performed on an Intel Pentium IV workstation equipped with Linux Redhatver. 7.3.

5.7.2. Clog *P* for compounds 1–15. The log *P* values of the examined compounds were calculated using the Daylight computational method (version 4.01) that combines fragment lipophilicity contributions carefully parameterized with experimental data and calculated 'from scratch' values.²²

5.7.3. Pharmacophore modeling. All computations were performed with Catalyst 4.9 on an Indigo O2 Workstation (255 MHz, MIPS R10000, 320 MB RAM) running Irix 6.5. Conformational models were generated with the BEST option, a maximum number of 250 conformers per compound, and the default energy cutoff value of 20 kcal/mol. When compounds were tested as a mixture of optical stereoisomers (Series II), the relevant stereoisomers were drawn as sterically undefined. In this case, Catalyst automatically chooses the best fitting stereoisomer during model generation and fitting. The construction of the pharmacophore hypothesis for σ₁ has been reported previously.²⁷ The graphics in Figure 9 were created with WebLab Viewer Lite 3.5.³²

5.8. Radioligand binding study

The guinea pig brain membranes were prepared using the procedure described by Matsumoto et al.³³ Briefly,

guinea pig brain minus cerebella was homogenized in 10 volumes of ice-cold 0.32 M sucrose, pH 7.4, with a glass–Teflon homogenizer and then centrifuged at 3000 rpm for 10 min at 4 °C. The pellet was resuspended in 2 vol and centrifuged again at 3000 rpm for 10 min at 4 °C. The supernatants were collected and recentrifuged at 19,000 rpm for 20 min at 4 °C. The pellet was resuspended in 3 vol of 10 mM Tris–HCl, pH 7.4, incubated for 15 min at room temperature, and centrifuged again at 19,000 rpm for 15 min at 4 °C. The final pellet was resuspended in 1.53 vol and frozen at –80 °C until use.

σ_1 binding assays were performed as described by DeHaven and co-workers.³⁴ Briefly, 1 mL of membrane suspension (500 μ g of protein) and 3 nM [³H](+)-pentazocine (28 Ci/mmol; $K_d = 1.6 \pm 0.3$ nM, $n = 3$) in 50 mM Tris–HCl (pH 7.4) were incubated with test compounds (from 10^{-5} to 10^{-11} M). Nonspecific binding was assessed in the presence of 10 μ M haloperidol. The reaction was performed for 150 min at 37 °C and terminated by filtering the solution through a Whatman GF/B glass fiber filter which had been presoaked for 1 h in a 0.5% poly(ethylenimine) solution. Filters were washed twice with 4 mL of ice-cold buffer.

σ_2 binding assays were carried out as reported by Mach et al.³⁵ Briefly, 0.5 mL of membrane suspension (360 μ g protein) with 3 nM [³H]DTG [1,3-di-2-tolyl-guanidine] (31 Ci/mM; $K_d = 15.3 \pm 0.6$ nM, $n = 3$ nM) in the presence of 400 nM (+)-SKF10,047 to block σ_1 sites was incubated with test compounds. Incubation was carried out in 50 mM Tris–HCl (pH 8.0) for 120 min at room temperature. Each assay was terminated by the addition of ice-cold 10 mM Tris–HCl, pH 8.0, followed by filtration through a Whatman GF/B glass fiber filter which had been presoaked for 1 h in a 0.5% poly(ethylenimine) solution. Filters were washed twice with 4 mL of ice-cold buffer. Nonspecific binding was defined using 5 μ M DTG. Inhibition constants (K_i values) for test compounds were calculated using the EBDA/LIGAND program, purchased from Elsevier/Biosoft.³⁶

References and notes

- Martin, W. R.; Eades, C. G.; Thompson, J. A.; Huppler, R. E.; Gilbert, P. E. *J. Pharmacol. Exp. Ther.* **1976**, *197*, 517–532.
- Skuza, G. *Polish J. Pharmacol.* **2003**, *55*, 923–934.
- Quirion, R.; Chicheportiche, R.; Contreras, P. C.; Johnson, K. M.; Lodge, D.; Tam, S. W.; Woods, J. H.; Zukin, S. R. *Trends Pharmacol. Sci.* **1987**, *10*, 444–446.
- Walker, J. M.; Bowen, W. D.; Walker, F. O.; Matsumoto, R. R.; de Costa, B.; Rice, K. C. *Pharmacol. Rev.* **1990**, *42*, 335–402.
- Quirion, R.; Bowen, W. D.; Itzhak, Y.; Junien, J. L.; Musacchio, J. M.; Rothman, R. B.; Su, T. P.; Tam, S. W.; Taylor, D. P. *Trends Pharmacol. Sci.* **1992**, *13*, 85–86.
- Hellewell, S. B.; Bruce, A.; Feinstein, G.; Orringer, J.; Williams, W.; Bowen, W. D. *Eur. J. Pharmacol.* **1994**, *268*, 9–18.
- Vilner, B. J.; John, C. S.; Bowen, W. D. *Cancer Res.* **1995**, *55*, 408–413.
- Itzhak, Y. *Sigma Receptors*; Academic Press: San Diego, CA, 1994.
- Hayashi, T.; Su, T. P. *CNS Drugs* **2004**, *18*, 269–284.
- Hanner, M.; Moebius, F. F.; Flandorfer, A.; Knaus, H. G.; Striessnig, J.; Kempner, E.; Glossmann, H. *Proc. Natl. Acad. Sci. U.S.A.* **1996**, *93*, 8072–8077.
- Teruo, Hayashi; Tsung-Ping, Su *CNS Drugs* **2004**, *18*, 269–284.
- Moebius, F. F.; Striessnig, J.; Glossmann, H. *Trends Pharmacol. Sci.* **1997**, *18*, 67–70.
- Bowen, W. D. *Pharm. Acta. Helv.* **2000**, *74*, 211–218.
- Maurice, T. *Drug News Perspect.* **2002**, *15*, 617–625.
- Tam, S. W.; Cook, L. *Neurobiology* **1984**, *81*, 5618–5621.
- Chien, C. C.; Pasternak, G. W. *J. Pharmacol. Exp. Ther.* **1994**, *271*, 1583–1590.
- Mei, J.; Pasternak, G. W. *J. Pharmacol. Exp. Ther.* **2002**, *300*, 1070–1074.
- Glennon, R. A.; Ablordeppey, S. Y.; Ismaiel, A. M.; El-Ashmawy, M. B.; Fischer, J. B.; Howie, K. B. *J. Med. Chem.* **1994**, *37*, 1214–1219.
- Gund, T. M.; Floyd, J.; Jung, D. *J. Mol. Graphics Modell.* **2004**, *22*, 221–230.
- Azzolina, O.; Collina, S.; Brusotti, G.; Rossi, D.; Callegari, A.; Linati, L.; Barbieri, A.; Ghislandi, V. *Tetrahedron: Asymmetry* **2002**, *13*, 1073–1081.
- Lipinski, C. A.; Lombardo, F.; Dominy, B. W.; Freeney, P. J. *Adv. Drug Delivery Rev.* **1997**, *23*, 3–25.
- Leo, A. J.; Hoekman, D. *Perspect. Drug Discovery Des.* **2000**, *18*, 19–38.
- Azzolina, O.; Collina, S.; Rossi, D.; Alcaro, S.; Ghislandi, V. Experimental and computational approaches to estimate the hydrophobicity of antinociceptive agents, First Magna Grecia Medicinal Chemistry Workshop on New Perspectives in Drug Research, Copanello, Catanzaro, Italy, 10–13 June 2001.
- Banik, B. K.; Barakat, K. J.; Wagle, D. R.; Manhas, M. S.; Bose, A. K. *J. Org. Chem.* **1999**, *64*, 5746–5753.
- Farrugia, L. J. *J. Appl. Crystallogr.* **1997**, *30*, 565.
- Catalyst 4.9, Accelrys Inc., San Diego, CA, <http://www.accelrys.com>, 2003.
- Laggner, C.; Schieferer, C.; Fiechtner, B.; Poles, G.; Hoffmann, R. D.; Glossmann, H.; Langer, T.; Moebius, F. F. *J. Med. Chem.* **2005**, *18*, 4754–4764.
- Mohamadi, F.; Richards, N. G. J.; Guida, W. C.; Liskamp, R.; Lipton, M.; Caufield, C.; Chang, G.; Hendrickson, T.; Still, W. C. *J. Comput. Chem.* **1990**, *11*, 440–467.
- Still, W. C.; Tempczyk, A.; Hawley, R. C.; Hendrickson, T. *J. Am. Chem. Soc.* **1990**, *112*, 6127–6129.
- Collina, S.; Loddo, G.; Barbieri, A.; Linati, L.; Alcaro, S.; Chimenti, P.; Azzolina, O. *Tetrahedron: Asymmetry* **2004**, *15*, 3601–3608.
- Chang, G.; Guida, W. C.; Still, W. C. *J. Am. Chem. Soc.* **1989**, *111*, 4379–4386.
- WebLab Viewer Lite 3.5; Accelrys (Molecular Simulations Inc.): San Diego, CA, 1999.
- Matsumoto, R. R.; Bowen, W. D.; Tom, M. A.; Vo, V. N.; Truong, D. D.; De Costa, B. R. *Eur. J. Pharmacol.* **1995**, *280*, 301–310.
- DeHaven-Hudkins, D. L.; Ford-Rice, Y. *Eur. J. Pharmacol.* **1992**, *227*, 371–378.
- Macath, R. H.; Smith, C. R.; Childers, S. R. *Life Sci.* **1995**, *57*, 57–62.
- McPherson, G. A. *J. Pharmacol. Methods* **1985**, *14*, 213–228.